Strong Similarities in the Local Hydration Environments of the Bromide Ion and the $Cl^-\cdot CCl_3^\bullet$ Ion−Radical Complex: Factors Contributing to Intramolecular Distortions in the Primary Hydration Shell

William H. Robertson, Gary H. Weddle, and Mark A. Johnson*

Sterling Chemistry Laboratory, Yale University, P.O. Box 208107, New Haven, Connecticut 06520-8107

Received: May 21, 2003

We report the infrared photofragmentation spectra of the $Cl^-\cdot CCl_3\cdot nH_2O$, $n = 1-3$ complexes and compare the observed pattern of OH stretching vibrations with those displayed by the $X^-\cdot nH_2O$, [X = Cl, Br] clusters. The predissociation spectra reveal hydrogen bonded networks in the di- and trihydrate clusters. Addition of the $CCl_3^\bullet$ radical to the $Cl^-\cdot nH_2O$ complexes causes a significant blue shift in the OH stretching vibrations involving the hydrogen atoms bound to the ion. As a result, the $Cl^-\cdot CCl_3\cdot nH_2O$ spectra appear remarkably similar to those observed previously for the bromide hydrates. We trace this effect to partial charge delocalization onto the $CCl_3^\bullet$ radical through an analysis of the electronic structure carried out with density functional calculations. Two important factors contributing to the ion-bound OH stretch frequencies are the radius, (r_i), and excess charge, (q_i), associated with the halide. The red shifts displayed by the water molecule in a number of halide−water complexes are found to be strongly correlated with the parameter q_i/r_i^2, which accounts for both effects through their contributions to the electric field at the surface of the ion.

I. Introduction

Recent advances in cluster ion source technology[1] have created new opportunities to study how the binary anion−water interaction[2−5] is modified by the presence of a second molecule which can competitively bind to the ion. In an earlier report,[6] we followed the evolution of the $Cl^-\cdot H_2O$ mid-IR spectrum upon sequential addition of carbon tetrachloride molecules in a study of the $Cl^-\cdot nCCl_4\cdot H_2O$ clusters. The basic observation was that the CCl_4 molecules acted to weaken the $Cl^-\cdot H_2O$ interaction, as evidenced by a large incremental reduction in the red shift of the ionic H-bonded OH stretch in these asymmetric, single ionic H-bonded (SIHB) monohydrates.[7] This effect was traced to competitive charge-transfer such that excess charge is redistributed onto the CCl_4 molecules. As a result, the $Cl^-\cdot CCl_4\cdot H_2O$ spectrum in the OH stretching region appears remarkably similar to that of the more weakly bound (compared to $Cl^-\cdot H_2O$) $Br^-\cdot H_2O$ complex.[4] With the behavior of the $Cl^-\cdot nCCl_4\cdot H_2O$ system in mind, we present in this report the spectrum of the $Cl^-\cdot CCl_3\cdot H_2O$ complex to elucidate how an open shell partner participates in the competition for the excess charge. We then extend this study to follow additional of the second and third water molecules and therefore explore how the bulky $Cl^-\cdot CCl_3^\bullet$ complex anion affects the growth of attached water networks.[2]

II. Experimental Section

Infrared predissociation spectra were obtained with the Yale negative ion photofragmentation spectrometer described previously.[8] Briefly, bare and argon-solvated negative ions were produced by seeding carbon tetrachloride in an argon supersonic expansion, which was ionized by a counterpropagating 1 keV electron beam. The $Cl^-\cdot CCl_3^\bullet$ ion-radical complex central to this study is itself an interesting species, and it is efficiently formed using our argon-cluster mediated synthesis technique.[9−11] In this method, ions which are unstable with respect to dissociative electron attachment (DA) in an isolated electron−molecule collision can be stabilized by exploiting the "cage effect",[12,13] which becomes operative when DA occurs in moderately large argon clusters. Our approach is a variation on a cluster technique first reported by Klots and Compton[14] who produced CCl_4^- by electron attachment to CCl_4-doped CO_2 clusters, and later used by Schermann and Illenberger to synthesize NF_3^-.[15] We have previously employed this technique[16] to determine the structure of the methylene bromide and methyl iodide anions using predissociation spectroscopy in the C−H stretching range. Both cases are best described as a halide anion attached to one of the hydrogen atoms of the neutral radical fragment ($I^-\cdot HCH_2\cdot$ and $Br^-\cdot HCHBr\cdot$), leaving the unpaired electron localized primarily on the carbon atom.

The hydrated clusters were formed by evaporative condensation of water molecules onto $Cl^-\cdot CCl_3\cdot n$Ar clusters, where about six argon atoms are ejected for each absorbed water molecule. Water vapor is introduced on the low-pressure side of the expansion orifice by pulsed entrainment using our "supersonic-afterglow" arrangement,[11] which generates the distribution of cluster ions displayed in Figure 1. In a typical experiment, the steady-state pressure in the source chamber increased from 2×10^{-5} to 4×10^{-5} Torr upon introduction of the water vapor. Since the clusters suffer many evaporation events before extraction into the mass spectrometer, their internal energies should conform to the expected behavior of the "evaporative ensemble."[17] As such, the cluster internal energy is governed by the binding energy (D_o) of the most labile ligand. The argon-solvated clusters ($D_o(Cl^-\cdot Ar) \sim 600$ cm^{-1})[18] therefore have considerably lower internal energy than the $Cl^-\cdot CCl_3^\bullet$-based clusters ($D_o(Cl^-\cdot CCl_3^\bullet) \sim 4000$ cm^{-1})[19] which, in turn, contain less energy than the bare $Cl^-\cdot H_2O$ complex ($D_o(Cl^-\cdot H_2O) \sim 5200$ cm^{-1}).[20]

* To whom correspondence should be addressed.

10.1021/jp030641r CCC: $25.00
Published on Web 10/15/2003

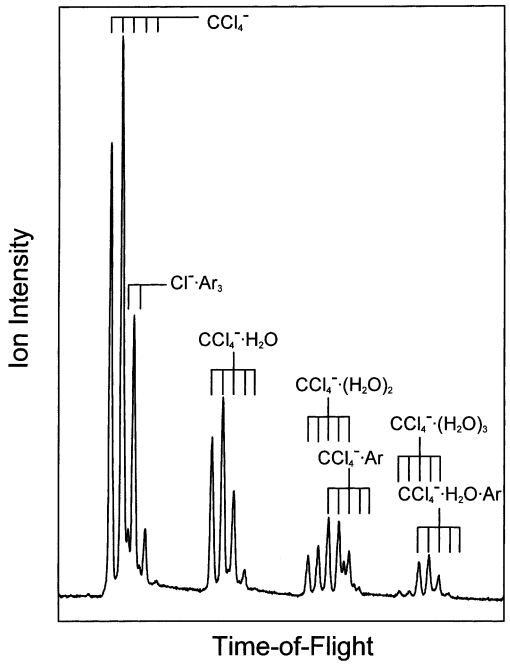

Figure 1. Mass spectrum resulting from trace CCl_4 seeded in an electron beam-ionized argon supersonic expansion, with H_2O introduced by pulsed entrainment[11] of neat water vapor on the low-pressure side of the 0.5 mm orifice.

To obtain their vibrational spectra, mass-selected clusters were irradiated with a pulsed infrared laser beam prior to isolation of the photofragment ions with the secondary (reflectron) mass spectrometer. This direct determination of both the parent and daughter ion masses allowed unambiguous stoichiometric identification of the spectral carrier even in cases when accidental mass coincidences (i.e., isobaric ions) precluded isolation of parents given the modest resolution ($M/\Delta M \approx 200$) of the primary mass spectrometer. The infrared radiation was provided by a Nd:YAG (Spectra Physics DCR-3) pumped, KTP/KTA-based OPO/OPA (LaserVision), which yielded ~5 mJ/pulse in the 2400−3800 cm^{-1} range. The spectra were corrected for laser fluence over the scan range.

Geometry optimizations and harmonic frequency calculations were performed at the B3LYP/aug-cc-pVDZ level as implemented in the Gaussian98 package.[21] The OH stretching frequencies were scaled by 0.9574 to bring the calculated ionic H-bonded OH stretch (OH_{IHB}) frequency in the $Cl^-\cdot CCl_4\cdot H_2O$ cluster into agreement with experiment. The $Cl^-\cdot CCl_4\cdot H_2O$ cluster, with only one low lying isomeric form, provides a convenient internal calibration for this anharmonic correction. Application of an analogous procedure to the intramolecular water bending mode yields a scaling factor of 0.9831.

III. Results and Discussion

A. On the Structure of the CCl_4^- Anion. Two isomeric forms of the CCl_4^- anion have been described in the literature using a combination of methods including dissociative electron attachment (DA),[14,22] ion−molecule kinetics,[23] low-temperature ESR,[24,25] matrix isolation spectroscopy,[19,26] and electronic structure theory.[19,27,28] The C_{3v} isomer, derived from the tetrahedral neutral structure by elongation of one C−Cl bond, was characterized by ESR[24,25] in tetramethylsilane and carbon tetrachloride matrices.[27,28] On the other hand, infrared spectroscopy of CCl_4^- in argon[19] and neon[26] matrices indicates the presence of an additional form where the chloride ion attaches to one of the chlorine atoms of the radical in a $Cl^-\cdot ClCCl_2^\bullet$ configuration.[26] Because the $CCl_3^\bullet$ radical is a nonplanar C_{3v} species, the $Cl^-\cdot ClCCl_2^\bullet$ arrangement occurs with C_s symmetry (as opposed to the C_{2v} geometry found in the $I^-\cdot CH_3^\bullet$ system). Richter et al.[19] have calculated that these structures are close in energy, with the C_{3v} structure lying about 300 cm^{-1} lower than the C_s form.

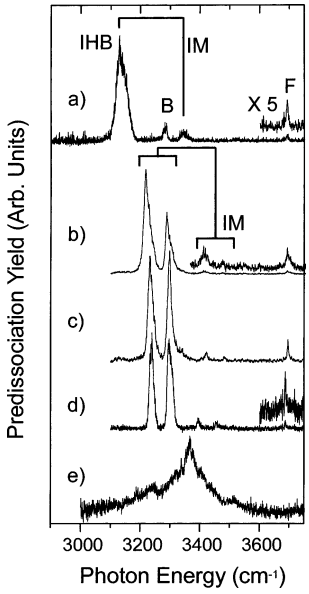

Figure 2. Comparison of the monohydrate infrared predissociation spectrum of $Cl^-\cdot CCl_3$ with those of various related anions: (a) $Cl^-\cdot H_2O\cdot 3Ar$,[4] (b) $Cl^-\cdot CCl_3\cdot H_2O$, (c) $Cl^-\cdot CCl_4\cdot H_2O$,[6] (d) $Br^-\cdot H_2O\cdot 3Ar$,[4] and (e) $Br^-\cdot H_2O$.[43] Note the dramatic response of the $Br^-\cdot H_2O$ spectrum to internal energy by comparison of the spectum arising from predissociation of a water molecule (trace e) to that obtained by loss of an argon atom (trace d). The labels F and IHB indicate the free and ionic H-bonded OH stretch fundamentals, respectively. The HOH intramolecular bending overtones are designated B. The brackets in parts a and b denote the combination band arising from excitation of the ion−water stretch soft mode (IM) along with the OH_{IHB} fundamental.

The photochemical behavior observed in this study is consistent with the basic identification of CCl_4^- to be a $CCl_3^\bullet$ radical weakly bound to Cl^-, as we observe mid-IR photoevaporation of $CCl_3^\bullet$ in the argon-free CCl_4^- hydrates, whereas no fragmentation is observed for bare $Cl^-\cdot H_2O$. Addition of the first argon atom completely suppresses $CCl_3^\bullet$ ejection, with argon loss providing the only fragmentation pathway upon excitation of $Cl^-\cdot CCl_3\cdot H_2O\cdot Ar$ in the 3200 cm^{-1} range. This indicates that $CCl_3^\bullet$ is more strongly bound to the chloride anion than argon ($D_o(Cl^-\cdot Ar)$), in contrast to the situation in the methyl iodide anion.[16] In the latter case, $D_o(I^-\cdot CH_3\cdot)$ is on the same order as $D_o(I^-\cdot Ar)$, and methyl radical loss in fact dominates argon atom ejection upon excitation of the CH stretching fundamentals.

B. Infrared Predissociation Spectra of $Cl^-\cdot CCl_3\cdot nH_2O$ Anions. B1. $Cl^-\cdot CCl_3\cdot H_2O$. Figure 2 compares the $Cl^-\cdot CCl_3\cdot H_2O$ infrared spectrum with that of $Cl^-\cdot CCl_4\cdot H_2O$[6] and the argon predissociation spectra[4] of $Br^-\cdot H_2O$ and $Cl^-\cdot H_2O$. All four spectra (Figure 2a−d) display weak, sharp features near the mean of the symmetric and asymmetric stretches of an isolated water molecule (3707 cm^{-1}),[29] which are thus assigned to the free OH stretch fundamental (denoted F in Figure 2). This confirms that in each case, the water molecule is bound to the ion in the usual, single ionic H-bond (SIHB) configuration. The ionic H-bonded OH stretching (OH_{IHB}) bands are more interesting, evolving from a single dominant feature in $Cl^-\cdot H_2O$ to an asymmetric doublet in $Cl^-\cdot CCl_3\cdot H_2O$ and finally to a

TABLE 1: Deperturbed Band Origins[a] (±5 cm^{-1}) of OH_{IHB} Stretching and HOH Intramolecular Bending (2 ← 0) Overtone Vibrations in Addition to the Ion−Water Stretching Fundamentals Observed in Combination with $v = 1$ of the OH_{IHB} Stretches[e]

	OH_{IHB} stretch (cm^{-1})	bend overtone (B) (cm^{-1})	ion−water stretch[b] (cm^{-1})
$Cl^-\cdot H_2O$	3138 (3149)	3276 (3269)	210 (193)
$Cl^-\cdot CCl_3\cdot H_2O$	3238 (**I** = 3244, **II** = 3352, **III** = 3024)[c]	3265 (**I** = 3266, **II** = 3276, **III** = 3250)[c]	200 (**I** = 177, **II** = 165, **III** = 234)[c]
$Cl^-\cdot CCl_4\cdot H_2O$	3264[d]	3264[d]	186 (175)
$Br^-\cdot H_2O$	3270 (3271)	3264(3259)	158 (158)

[a] See text for details. [b] No scaling applied to harmonic frequencies for this mode. [c] Isomer designations (**I**, **II**, **III**) are defined in Figure 3. [d] Calculated harmonic frequencies scaled to these experimental values. [e] Scaled harmonic frequencies[a] (calculated at the B3LYP/aug-cc-pVDZ level) are given in parentheses.

symmetric doublet in the $Cl^-\cdot CCl_4\cdot H_2O$ and $Br^-\cdot H_2O$ cases. This strong doubling has been assigned[4,6] to a Fermi-type coupling between the $v = 1$ level of the OH_{IHB} stretch and the $v = 2$ level of the intramolecular bending overtone of water. The similarity of the OH stretching spectra in the three different systems (Figure 2b−d) clearly indicates that the H_2O intramolecular dynamics are relatively insensitive to the exact chemical nature of the nearby ion. Below we analyze the observed level positions to establish quantitative aspects of the ion−molecule interactions at play.

B.1.1. Assignment of the $Cl^-\cdot CCl_3^\bullet$ Complex Structure and Evaluation of the Ion Dependence of the Intramolecular Perturbation on the Water Molecule. We have confirmed the assignment of the strong doublet (Figure 1b−d) to a bend/stretch Fermi diad by observing (in all three cases) its collapse to a single feature in the $X^-\cdot HOD$ isotopomers.[6] This occurs because the bending overtone in HOD is shifted out of resonance with the OH_{IHB} fundamental. The relative intensities of the coupled IHB/B transitions within the doublet are determined by the amount of OH_{IHB} character in each mixed state. In the limiting case where the zero-order levels are accidentally degenerate, the two members of the diad appear with equal intensities and are split by twice the interaction matrix element. Thus, the peak spacing in a symmetrical doublet enables a particularly straightforward determination of the Fermi matrix element, and this circumstance is realized in the $Br^-\cdot H_2O$ and $Cl^-\cdot CCl_4\cdot H_2O$ spectra. Interestingly, the $Br^-\cdot H_2O$ cluster displays a distinctly smaller interaction matrix element (30 cm^{-1}) than that of the $Cl^-\cdot CCl_4\cdot H_2O$ cluster (33 cm^{-1}), despite the fact that their OH stretching and bending overtone level positions are nearly identical. Note that the Fermi interaction in $Cl^-\cdot H_2O$, which occurs between the more distant zero-order levels, is also described by the larger 33 cm^{-1} matrix element which characterizes the $Cl^-\cdot CCl_x$ complexes.[6] By constraining the solutions of the diagonalized 2 × 2 Fermi Hamiltonian to recover the observed splittings and relative band intensities, we extracted the deperturbed OH stretch and bending overtone level positions with the results collected in Table 1.

Comparisons of the deperturbed band origins with calculated fundamentals are useful in assigning the isomeric form of the $Cl^-\cdot CCl_3\cdot H_2O$ complexes generated in the ion source. Geometry optimizations, carried out at the B3LYP/aug-cc-pVDZ level, recovered the three local minima for $Cl^-\cdot CCl_3\cdot H_2O$ (denoted **I**, **II**, and **III**) depicted in Figure 3, along with the structure of the previously reported[6] $Cl^-\cdot CCl_4\cdot H_2O$ complex. Isomers **I** and **II** are formed by attachment of a water molecule to the two isomers of the $Cl^-\cdot CCl_3$ radical anion discussed above, while isomer **III** results from insertion of the water molecule between the radical and the chloride anion. Calculated vibrational frequencies for each isomer are collected in Table 1.

Isomer **I**, derived from the $Cl^-\cdot ClCCl_2^\bullet$ anion, has a calculated OH_{IHB} fundamental (3243 cm^{-1}) in excellent agreement with that observed experimentally (3238 cm^{-1}), whereas isomer **II**, derived from the C_{3v} $Cl^-\cdot CCl_3^\bullet$ anion, is predicted to display an OH_{IHB} stretch about 100 cm^{-1} above the deperturbed OH_{IHB} band origin. The calculated spectrum of the "insertion" structure **III** is in poorest agreement with the observed spectrum, with its predicted OH_{IHB} fundamental lying 200 cm^{-1} below the observed transitions.

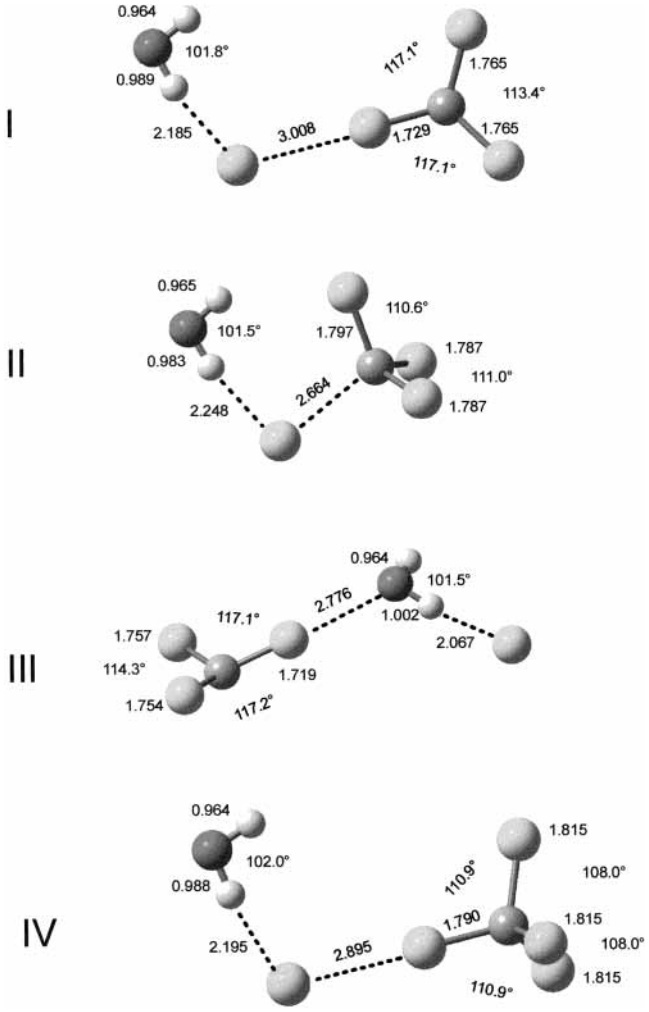

Figure 3. Optimized structures of $Cl^-\cdot CCl_3\cdot H_2O$ (**I**, **II**, and **III**) and $Cl^-\cdot CCl_4\cdot H_2O$ (**IV**) calculated at the B3LYP/aug-cc-pVDZ level. Bond distances and angles are given in angstroms and degrees, respectively.

B.1.2. Development of a Local Field Parameter as an Empirical Index for the OH_{IHB} Red Shifts. The similarity of the OH_{IHB} red shift displayed by the $Br^-\cdot H_2O$, $Cl^-\cdot CCl_3\cdot H_2O$, and $Cl^-\cdot CCl_4\cdot H_2O$ complexes suggests that the local environment of the water molecule is somehow equivalent despite the larger radius,[30] r_i, of the bromide ion (1.96 Å) relative to that of chloride (1.81 Å). One issue raised previously in our discussion of the $Cl^-\cdot nCCl_4\cdot H_2O$ complexes is the fact that attachment of a chlorinated solvent molecule to chloride acts

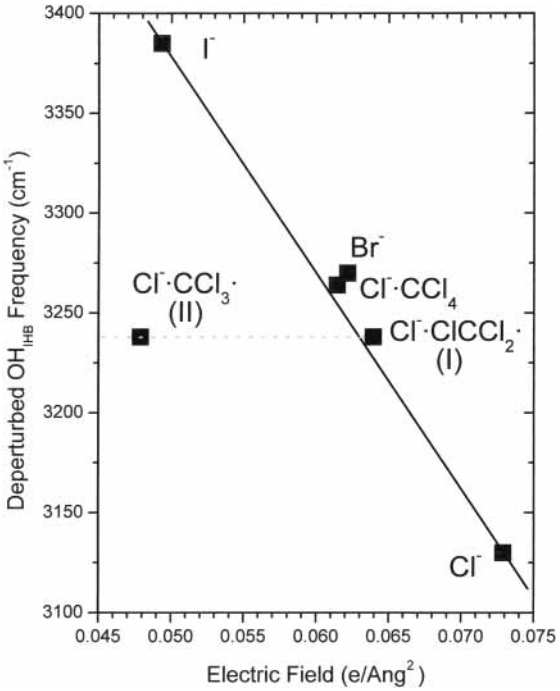

Figure 4. Deperturbed ionic H-bonded OH stretching frequencies (Table 1) for monohydrates plotted as a function of approximate electric field due to the halide, defined as indicated in the text. Note that the field calculated for the $Cl^-\cdot ClCCl_2$ anion structure present in isomer **I** brings much better agreement with the trend established by the halides than that calculated for the $Cl^-\cdot CCl_3$ anion (leading to isomer **II**).

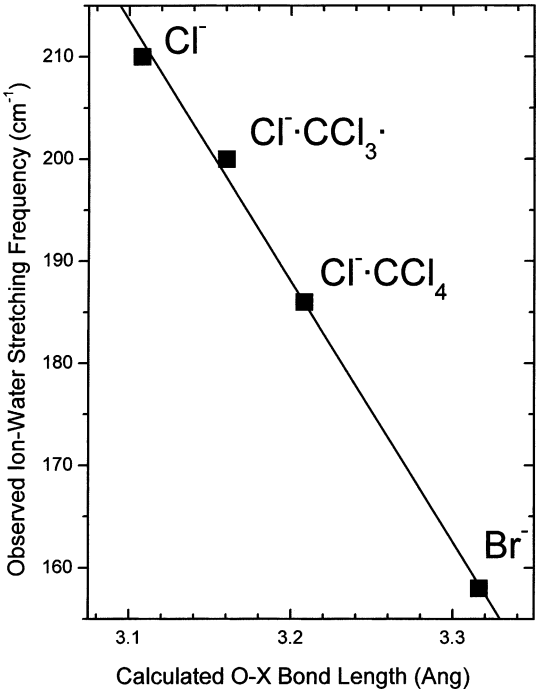

Figure 5. Badger's rule plot of observed ion−water stretching frequency in $X^-\cdot H_2O$ complexes as a function of calculated O−X distance. Ion−water stretching frequencies are from this work and refs 4 and 6. The O−Cl and O−Br distances are taken from ref 45.

to reduce the effective charge on the halide. Indeed, in both the $Cl^-\cdot CCl_3\cdot H_2O$ and $Cl^-\cdot CCl_4\cdot H_2O$ complexes, simple Mulliken charge (q_m) analysis indicates substantial charge redistribution onto the CCl_x moiety. More excess charge appears on the CCl_4 molecule (0.124 *e*) than on the $CCl_3^\bullet$ radical in isomer **I** (0.086 *e*), while isomer **II** accommodates more excess charge (0.255 *e*) than CCl_4.

These electronic structure calculations suggest that reduction in local excess charge associated with the halide in the $Cl^-\cdot CCl_x$ complexes compensates for the smaller inherent radius of Cl^- relative to Br^- such that both species similarly distort an attached H_2O molecule. An obvious way to express this effect is to estimate the local electric field in the vicinity of the anion (E_X) according to q_m/r_i^2. For purposes of discussion, we fixed r_i at the halide crystal radii and took q_m to be a unit charge for the bare halide ion monohydrates and assigned Mulliken charges for q_m in the $Cl^-\cdot CCl_x\cdot H_2O$ systems. These charges were extracted from calculations on the bare $Cl^-\cdot CCl_x$ complexes, so that this field parameter characterizes the environment around the ion before introduction of the water molecule, which is known[2] to further participate in charge delocalization via intracluster proton transfer. Figure 4 presents a plot of the observed OH_{IHB} red shifts as a function of this crude field parameter, indicating that the observed trend can indeed be qualitatively understood on this basis.[31,32] The field dependence established by the bare halides clearly supports the assignment of the $Cl^-\cdot CCl_3\cdot H_2O$ complex formed in the ion source to isomer **I**.

B.1.3. Complex Dependence of the Water—Ion Stretching Soft Mode. Another aspect of the local solvation environment around the anion concerns the strength of the H-bonds to the water molecule. This is reflected in the spectra by the energy of the ion−water stretching soft modes that accompany the OH_{IHB} transitions as combination bands (IM in Figure 2). These combination bands appear when the water molecule becomes more tightly bound in the OH_{IHB} vibrationally excited state, which shifts the vibrationally adiabatic potentials governing this soft mode in the OH $v = 0$ and $v = 1$ stretching levels.[33,34] The energy of this soft mode vibration is observed to be dependent on the halide ion,[4] with the behavior of the $Cl^-\cdot CCl_x$ complexes falling between the limiting behavior of the $Cl^-\cdot H_2O$ and $Br^-\cdot H_2O$ systems as is evident by close inspection of Figure 2. To display this dependence more clearly, we plot in Figure 5 the observed soft mode frequencies against calculated X−O distances (using literature values[35] where available and supplementing these with our own calculations for the $Cl^-\cdot CCl_x$ complexes, which have not been reported previously). On a qualitative level, the addition of either CCl_4 or $CCl_3^\bullet$ to the $Cl^-\cdot H_2O$ complex leads to a weakening of the $Cl^-\cdot H_2O$ interaction, which is reflected in a softening of the $Cl^-\cdots H_2O$ stretching vibration and, as noted above, a reduction of the OH_{IHB} red shift. This establishes that longer ion···water molecule distances correlate with lower frequencies of the ion−molecule stretching soft mode, as might be anticipated from a Badger's rule type of empirical relationship. Interestingly, although the OH_{IHB} fundamentals of the $Br^-\cdot H_2O$ and $Cl^-\cdot CCl_4\cdot H_2O$ complexes are almost identical, the energy of the chloride complex soft mode is still significantly above that found in $Br^-\cdot H_2O$ (by $\sim$30 cm^{-1}).

B.1.4. Crude Control of Internal Energy and Argon Dependence of the Band Contours. As discussed in section II, the internal energy of the $Cl^-\cdot CCl_3\cdot H_2O$ complex falls between that of the argon-solvated $Cl^-\cdot CCl_3\cdot H_2O\cdot n$Ar complexes and the bare halide−water complexes. This intermediate temperature regime is evidenced in the $Cl^-\cdot CCl_3\cdot H_2O$ spectrum (Figure 2b) by retention of the IHB/B doublet, a feature which is completely lost in the $Br^-\cdot H_2O$ spectrum (Figure 2e), where water monomer predissociation samples clusters with largest internal excitation.[36] On a more detailed level, the residual internal excitation in the $Cl^-\cdot CCl_3\cdot H_2O$ complex is revealed by hot-band structure which acts to distort the doublet with a

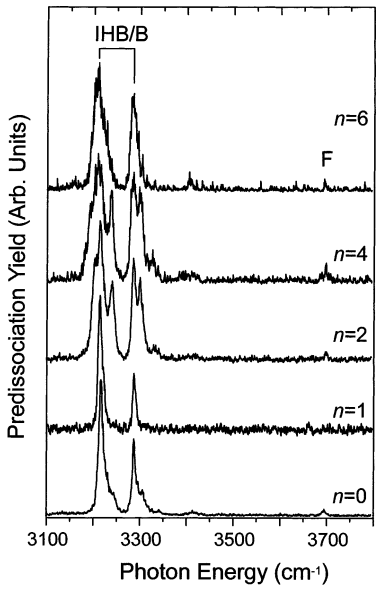

Figure 6. Infrared predissociation spectra of $Cl^-\cdot CCl_3\cdot H_2O\cdot nAr$ ($n = 0-2,4,6$). IHB/B denotes the mixed ionic H-bonded OH stretch/intramolecular water bending overtone transitions. F denotes the free OH stretch. The $n = 0$ spectrum was obtained by $CCl_3^\bullet$ predissociation while the $n > 0$ spectra were recorded by argon predissociation.

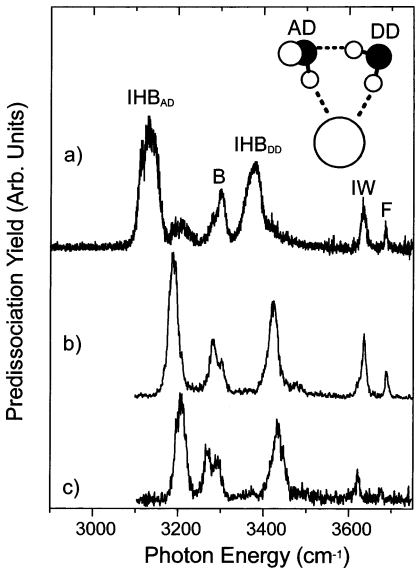

Figure 7. Comparison of the dihydrate predissociation spectra: (a) $Cl^-\cdot 2H_2O\cdot 3Ar$,[38] (b) $Cl^-\cdot CCl_3\cdot 2H_2O\cdot Ar$, and (c) $Br^-\cdot 2H_2O\cdot 3Ar$.[38] Inset structure depicts the arrangement of the water network implied by the OH band patterns. IHB_{AD} and IHB_{DD} denote the ionic H-bonded OH stretches on the acceptor−donor (AD) and double-donor (DD) water molecules, respectively. The labels F and IW indicate the free and inter-water H-bonded OH stretch fundamentals, respectively. The intramolecular water bending overtones are designated B.

blue-degradation of both IHB/B band envelopes. Note that this distortion disappears upon addition of one argon atom (Figure 6, $n = 0$ and $n = 1$). This blue-degradation is typical of the $\Delta v = 0$ sequence band structure based on the ion−water stretching soft mode.[37] Figure 6 also includes the evolution of the bands with attachment of additional argon atoms to establish the sensitivity of our conclusions to the extent of argon solvation. Some argon-dependent fine structure is observed on the IHB/B band envelopes (Figure 6, $n = 2-6$), much like that previously analyzed[34,37] in the $Cl^-\cdot H_2O\cdot(1-13)Ar$ and $I^-\cdot ROH\cdot(1-7)Ar$ (R = methyl, ethyl, isopropyl) systems. The previous analysis attributed the similar small splittings[34,37] to coexisting isomeric arrangements of the argon atoms in the primary solvation shell, which is typically filled in the size range $n \sim 10$.

B.2.The Second Water Molecule: $Cl^-\cdot CCl_3\cdot 2H_2O$. The $Cl^-\cdot CCl_3\cdot 2H_2O$ spectrum is presented in Figure 7 along with the previously reported[38] $Cl^-\cdot 2H_2O$ and $Br^-\cdot 2H_2O$ spectra to emphasize the pattern similarities, including minor features. This allows assignment of the bands by inspection based on the previous analyses of the halide dihydrates (Cl, Br, and I).[2,9,38] An intact water dimer adopts a cyclic structure with each water molecule H-bonded to the anion as well as to each other. The two water molecules are asymmetric, with one adopting an acceptor−donor (AD) and the other a double-donor (DD) H-bonding configuration (Figure 7 inset). The two ionic H-bonds, denoted IHB_{AD} and IHB_{DD}, occur at 3190 and 3425 cm^{-1}, respectively (Figure 7b). The water molecule in the AD configuration gives rise to the largest red shift because its ionic H-bond is cooperatively enhanced by accepting an inter-water H-bond (IW).[38−40] The formation of an inter-water (IW) H-bond is established by the appearance of the characteristic[38] IW band at 3635 cm^{-1}. The sharp band near 3692 cm^{-1} is due to the free OH on the AD water molecule, while the structured feature centered at 3285 cm^{-1} is assigned to overtones of the intramolecular water bending modes. The occurrence of two bands associated with the bending overtones reflects the fact that bending mode depends on the local environment of a water molecule, with the DD water molecule displaying a higher harmonic frequency than that of the water molecule in the AD configuration. Thus, the higher energy member of the doublet arises from mixing with the more distant IHB_{DD} fundamental, and is consequently weaker as it acquires less OH stretch character in the intensity borrowing mechanism. Note that this trend is reversed in the more red-shifted $Cl^-\cdot 2H_2O$ spectrum (Figure 7a).

To examine the evolution of the band locations in the dihydrate complexes, we again turn to the approximate field (E_X) parametrization presented in section III.B1.2 (and Figure 4) as an index for the local solvation environment. Figure 8 presents the E_X dependence of the various OH stretching bands displayed by the dihydrate complexes. Note that the two OH_{IHB} bands (shown as squares and triangles) red shift with E_X, whereas the IW band (circles) blue shifts signifying a weakening of the IW H-bond. In the $Cl^-\cdot 2H_2O$ complex, for example, Xantheas[41,42] estimated that the IW H-bond strength is reduced to only about one-tenth the value found in the isolated neutral water dimer.

The delicate nature of the IW H-bond is also evident in the argon dependence of the $Cl^-\cdot CCl_3\cdot 2H_2O$ spectra presented in Figure 9. The elevated internal excitation of the $Cl^-\cdot CCl_3\cdot 2H_2O$ cluster (relative to the argon containing clusters) is evidenced by the presence of two broad new features at 3245 and 3330 cm^{-1}, which are likely due to clusters containing sufficient internal energy to elongate or dissociate the IW H-bond. The extra bands promptly disappear upon addition of the first argon atom (Figure 9, $n = 1$). In contrast to the halide hydrates,[38,43] the internal energy limit provided by $CCl_3^\bullet$ evaporation is sufficiently low to allow the bare $Cl^-\cdot CCl_3\cdot 2H_2O$ cluster ensemble to contain a large fraction of intact water dimer subunits as is evidenced by the persistence of the 3635 cm^{-1} IW band (Figure 9, $n = 0$).

B.3. The Third Water Molecule: $Cl^-\cdot CCl_3\cdot 3H_2O$. The infrared $CCl_3^\bullet$ predissociation spectrum of the $Cl^-\cdot CCl_3\cdot 3H_2O$ complex is shown in Figure 10 and is compared to the argon predissociation spectra of $Cl^-\cdot 3H_2O$ and $Br^-\cdot 3H_2O$. All three spectra in Figure 10 arise from homodromic[39] water trimer

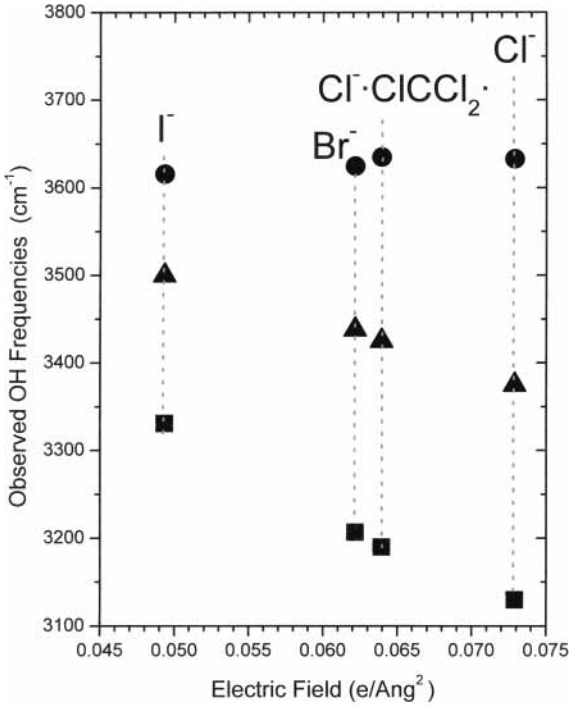

Figure 8. Observed OH stretching fundamentals for various anion dihydrates plotted as a function of approximate electric field due to the halide (see text). The squares (■) and triangles (▲) denote ionic H-bonded OH stretches of the acceptor−donor and double-donor water molecules, respectively. The circles (●) refer to the inter-water H-bonded OH stretches.

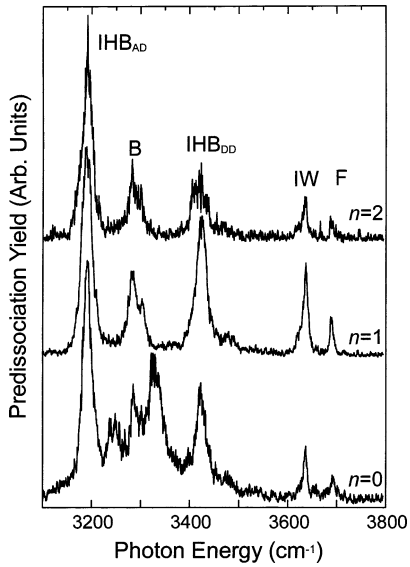

Figure 9. Argon solvation dependence of the $Cl^-\cdot CCl_3\cdot 2H_2O\cdot n$Ar ($n = 0-2$) predissociation spectra. Note the extra bands in the $n = 0$ case. See the caption of Figure 7 for label definitions.

subunits, where each water molecule is involved in one IHB and two IW H-bonds in a donor−donor−acceptor (DDA) H-bonding arrangement (see inset). The absence of a free OH stretch in the 3700 cm^{-1} region confirms the cyclic DDA assignment. Formation of the $(H_2O)_3$ trimer in $Cl^-\cdot CCl_3\cdot 3H_2O$ gives rise to two groups of OH stretching modes: IW ring modes near 3600 cm^{-1} and IHB modes centered at 3400 cm^{-1}. The appearance of the water bending modes at higher frequency in the $Cl^-\cdot CCl_3\cdot 3H_2O$ system relative to the monohydrate is consistent with the calculated behavior[41] of the bending frequencies of DDA-bonded water molecules in the $Cl^-\cdot nH_2O$ system.

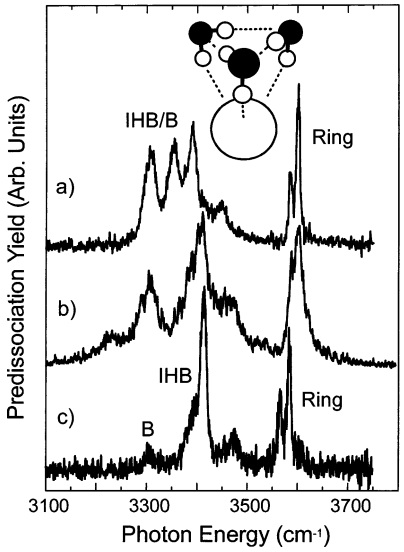

Figure 10. Comparison of the trihydrate predissociation spectra: (a) $Cl^-\cdot 3H_2O\cdot 3Ar$,[46] (b) $Cl^-\cdot CCl_3\cdot 3H_2O$, and (c) $Br^-\cdot 3H_2O\cdot 3Ar$.[46] Inset structure depicts the arrangement of the water network implied by the OH band patterns. Ring denotes inter-water H-bonded OH stretching ring-mode fundamentals, IHB refers to the ionic H-bonded OH stretching fundamentals, and B indicates intramolecular bending overtones.

The IW ring modes appear as a poorly resolved doublet in the $Cl^-\cdot CCl_3\cdot 3H_2O$ spectrum as compared to the well-defined ~2:1 doublet structure seen in the $X^-\cdot 3H_2O$ spectra (X = Cl, Br, I).[38] The broadening of the IW doublet in the $Cl^-\cdot CCl_3\cdot 3H_2O$ spectrum may be a thermal effect, but may also arise because the C_3 symmetry of the water trimer is perturbed by the C_s structure of the $Cl^-\cdot ClCCl_2\cdot$ anion. Argon predissociation spectra of $Cl^-\cdot CCl_3\cdot 3H_2O$ were not collected due to difficulties in producing the tagged clusters in sufficient quantity.

IV. Summary

We have presented infrared predissociation spectra of mass-selected hydrates of the $Cl^-\cdot CCl_3\bullet$ complex anion and interpreted the observed vibrational band patterns in the context of the previously reported halide hydrates. The $Cl^-\cdot CCl_3\bullet$ anion is found to be a weakly bound ion-radical complex that exhibits halide-like H-bonding behavior, distorting the hydrate subclusters slightly more than the Br^- anion. This is rationalized in terms of charge delocalization from the Cl^- anion onto the $CCl_3\bullet$ radical. Interestingly, the open-shell $CCl_3\bullet$ radical perturbs the $Cl^-\cdot H_2O$ spectrum *less* than the closed shell CCl_4 molecule.

Acknowledgment. We thank the Chemistry Division of the National Science Foundation for generous support of this work.

References and Notes

(1) Duncan, M. A. *Int. J. Mass. Spectrom.* **2000**, *200*, 545.

(2) Robertson, W. H.; Johnson, M. A. Molecular aspects of halide ion hydration: the cluster approach. *Annu. Rev. Phys. Chem.* **2003**, *54*, 173−213.

(3) Johnson, M. S.; Kuwata, K. T.; Wong, C.-K.; Okumura, M. *Chem. Phys. Lett.* **1996**, *260*, 551.

(4) Ayotte, P.; Weddle, G. H.; Kim, J.; Johnson, M. A. *J. Am. Chem. Soc.* **1998**, *120*, 12361.

(5) Ayotte, P.; Kelley, J. A.; Nielsen, S. B.; Johnson, M. A. *Chem. Phys. Lett.* **2000**, *316*, 455.

(6) Robertson, W. H.; Weddle, G. H.; Kelley, J. A.; Johnson, M. A. *J. Phys. Chem. A* **2002**, *106*, 1205.

(7) Thompson, W. H.; Hynes, J. T. *J. Am. Chem. Soc.* **2000**, *122*, 6278.

(8) Johnson, M. A.; Lineberger, W. C. Pulsed methods for cluster ion spectroscopy. In *Techniques for the Study of Gas-Phase Ion Molecule Reactions*; Saunders, W. H., Farrar, J. M., Eds.; Techniques of Chemistry; Wiley: New York, 1988; Vol. XX, Chapter XI, p 591.

(9) Ayotte, P.; Weddle, G. H.; Kim, J.; Johnson, M. A. *Chem. Phys.* **1998**, *239*, 485.

(10) Kim, J.; Kelley, J. A.; Ayotte, P.; Nielsen, S. B.; Weddle, G. H.; Johnson, M. A. *J. Am. Soc. Mass Spectrom.* **1999**, *10*, 810.

(11) Robertson, W. H.; Kelley, J. A.; Johnson, M. A. *Rev. Sci. Instrum.* **2000**, *71*, 4431.

(12) Papanikolas, J. M.; Vorsa, V.; Nadal, M. E.; Campanola, P. J.; Buchenau, H. K.; Lineberger, W. C. *J. Chem. Phys.* **1993**, *99*, 8733.

(13) Papanikolas, J. M.; Gord, J. R., Jr.; Levinger, N. E.; Ray, D.; Vorsa, V.; Lineberger, W. C. *J. Phys. Chem.* **1991**, *95*, 8028.

(14) Klots, C. E.; Compton, R. N. *J. Chem. Phys.* **1977**, *67*, 1779.

(15) Ruckhaberle, N.; Lehmann, L.; Matejcik, S.; Illenberger, E.; Bouteiller, Y.; Periquet, V.; Museur, L.; Desfrancois, C.; Schermann, J.-P. *J. Phys. Chem. A* **1997**, *101*, 9942.

(16) Nielsen, S. B.; Ayotte, P.; Kelley, J. A.; Weddle, G. H.; Johnson, M. A. *J. Chem. Phys.* **1999**, *111*, 10464.

(17) Klots, C. E. *J. Chem. Phys.* **1985**, *83*, 5854.

(18) Lenzer, T.; Yourshaw, I.; Furlanetto, M. R.; Pivonka, N. L.; Neumark, D. M. *J. Chem. Phys.* **2001**, *115*, 3578.

(19) Richter, A.; Meyer, H.; Muller, T.; Specht, H.; Schweig, A. *J. Mol. Struct.* **1997**, *436*−*437*, 359.

(20) *NIST Chemistry WebBook*; National Institute of Standards and Technology: Gaithersburg, MD, 2001.

(21) Frisch, M. J.; Trucks, G. W.; Schlegel, H. B.; Scuseria, G. E.; Robb, M. A.; Cheeseman, J. R.; Zakrzewski, V. G.; J. A. Montgomery, J.; Stratmann, R. E.; Burant, J. C.; Dapprich, S.; Millam, J. M.; Daniels, A. D.; Kudin, K. N.; Strain, M. C.; Farkas, O.; Tomasi, J.; Barone, V.; Cossi, M.; Cammi, R.; Mennucci, B.; Pomelli, C.; Adamo, C.; Clifford, S.; Ochterski, J.; Petersson, G. A.; Ayala, P. Y.; Cui, Q.; Morokuma, K.; Malick, D. K.; Rabuck, A. D.; Raghavachari, K.; Foresman, J. B.; Cioslowski, J.; Ortiz, J. V.; Baboul, A. G.; Stefanov, B. B.; Liu, G.; Liashenko, A.; Piskorz, P.; Komaromi, I.; Gomperts, R.; Martin, R. L.; Fox, D. J.; Keith, T.; Al-Laham, M. A.; Peng, C. Y.; Nanayakkara, A.; Challacombe, M.; Gill, P. M. W.; Johnson, B.; Chen, W.; Wong, M. W.; Andres, J. L.; Gonzalez, C.; Head-Gordon, M.; Replogle, E. S.; Pople, J. A. *GAUSSIAN 98*; Gaussian: Pittsburgh, PA, 1998.

(22) Matejcik, S.; Kiendler, A.; Stamatovic, A.; Mark, T. D. *Int. J. Mass. Spectrom. Ion Proc.* **1995**, *149/150*, 311.

(23) Staneke, P. O.; Groothuis, G.; Ingemann, S.; Nibbering, N. M. M. *Int. J. Mass. Spectrom. Ion Proc.* **1995**, *142*, 83.

(24) Bonazzola, L.; Michaut, J. P.; Roncin, J. *Chem. Phys. Lett.* **1988**, *153*, 52.

(25) Muto, H.; Nunome, K. *J. Chem. Phys.* **1991**, *94*, 4741.

(26) Lugez, C. L.; Jacox, M. E.; Johnson, R. D. J., III. *J. Chem. Phys.* **1998**, *109*, 7147.

(27) Gutsev, G. L. *J. Chem. Phys.* **1993**, *93*, 7072.

(28) Roszak, S.; Kaufman, J. J.; Koski, W. S.; Vijayakumar, M.; Balasubramanian, K. *J. Chem. Phys.* **1994**, *101*, 2978.

(29) Benedict, W. S.; Gailar, N.; Plyler, E. K. *J. Chem. Phys.* **1956**, *24*, 1139.

(30) *CRC Handbook of Chemistry and Physics*, 76th ed.; Lide, D. R., Ed.; CRC Press: New York, 1995.

(31) Hermansson, K. *Chem. Phys. Lett.* **1995**, *233*, 376.

(32) Hermansson, K. *J. Chem. Phys.* **1993**, *99*, 861.

(33) Weiser, P. S.; Wild, D. A.; Bieske, E. J. *Chem. Phys. Lett.* **1999**, *299*, 303.

(34) Nielsen, S. B.; Ayotte, P.; Kelley, J. A.; Johnson, M. A. *J. Chem. Phys.* **1999**, *111*, 9593.

(35) Kim, J.; Lee, H. M.; Suh, S. B.; Majumdar, D.; Kim, K. S. *J. Chem. Phys.* **2000**, *113*, 5259.

(36) Kelley, J. A.; Weber, J. M.; Lisle, K. M.; Robertson, W. H.; Ayotte, P.; Johnson, M. A. *Chem. Phys. Lett.* **2000**, *327*, 1.

(37) Corcelli, S. A.; Kelley, J. A.; Tully, J. C.; Johnson, M. A. *J. Phys. Chem.* **2002**, *106*, 4872.

(38) Ayotte, P.; Nielsen, S. B.; Weddle, G. H.; Johnson, M. A.; Xantheas, S. S. *J. Phys. Chem. A* **1999**, *103*, 10665.

(39) Xantheas, S. S. *Chem. Phys.* **2000**, *258*, 225.

(40) Robertson, W. H.; Karapetian, K.; Ayotte, P.; Jordan, K. D.; Johnson, M. A. *J. Chem. Phys.* **2002**, *116*, 4853.

(41) Xantheas, S. S. *J. Phys. Chem.* **1996**, *100*, 9703.

(42) Dorsett, H. E.; Watts, R. O.; Xantheas, S. S. *J. Chem. Phys. A* **1999**, *103*, 3351.

(43) Ayotte, P.; Bailey, C. G.; Weddle, G. H.; Johnson, M. A. *J. Phys. Chem. A* **1998**, *102*, 3067.

(44) Myshakin, E. M.; Jordan, K. D.; Robertson, W. H.; Weddle, G. H.; Johnson, M. A. *J. Chem. Phys.* **2003**, *118*, 4945.

(45) Hiraoka, K.; Mizuno, T.; Iino, T.; Eguchi, D. *J. Phys. Chem.* **2001**, *105*, 4887.

(46) Ayotte, P.; Weddle, G. H.; Johnson, M. A. *J. Chem. Phys.* **1999**, *110*, 7129.